IEEE Access
Multidisciplinary | Rapid Review | Open Access Journal

Received December 10, 2019, accepted February 3, 2020, date of publication February 11, 2020, date of current version February 19, 2020.

Digital Object Identifier 10.1109/ACCESS.2020.2973168

Design of Robust Higher-Order Repetitive Controller Using Phase Lead Compensator

MOHSIN JAMIL[1,2,3], (Senior Member, IEEE), ASIM WARIS[2], SYED OMER GILANI[2], (Senior Member, IEEE), BILAL A. KHAWAJA[1,4], (Senior Member, IEEE), MUHAMMAD NASIR KHAN[5], AND ALI RAZA[5]

[1]Department of Electrical Engineering, Faculty of Engineering, Islamic University of Madinah, Madinah 42351, Saudi Arabia
[2]Department of Robotics, School of Mechanical and Manufacturing Engineering (SMME), National University of Sciences and Technology (NUST), Islamabad 44000, Pakistan
[3]Department of Electrical and Computer Engineering, Faculty of Engineering and Applied Science, Memorial University of Newfoundland, St John's, NL A1B 35, Canada
[4]Department of Electronic and Power Engineering (EPE), PN-Engineering College (PNEC), National University of Sciences and Technology (NUST), Islamabad 44000, Pakistan
[5]Department of Electrical Engineering, University of Lahore, Lahore 54000, Pakistan

Corresponding author: Mohsin Jamil (drmohsin@ieee.org)

This work was supported by the Deanship of Scientific Research, Islamic University of Madinah, Kingdom of Saudi Arabia, under the Research Grant No. 28/40.

ABSTRACT The performance of conventional repetitive controller (RC) deteriorates under frequency variations and system uncertainties. Due to limited bandwidth, it is also a trivial task to stabilize the conventional RC. This paper proposes a higher-order repetitive controller (HORC) with linear phase lead as a stabilizing compensator and zero-phase tracking error (ZPTE) compensator. The periodic signal generator, used by the HORC, offers relatively high gains in the neighborhood of tuned frequency and its harmonics. Stability conditions for higher-order repetitive (HOR) control system, including the phase lead compensator, are presented. The proposed solution is applied to repetitive current control of a two-level grid-connected inverter. Simulation and experimental results show that the HORC designed using the phase lead compensation is robust to frequency variation in reference/disturbance and system uncertainties.

INDEX TERMS Repetitive controller, frequency variation, higher-order repetitive controller, phase lead.

I. INTRODUCTION

Repetitive controller (RC) offers the best performance over the reference tracking and disturbance rejection for periodic exogenous signals [1]. It is widely exploited in various application areas, e.g., power converters, active filters, multilink robotic manipulators, disk drives, power supplies, where high precision accuracy is required in the equipment [2]–[7]. The source of RC's high performance is that it offers very high gain at frequencies, which are multiples of the reference/disturbance signal frequency.

However, since the performance of the RC is significantly reduced for minimal variations in the reference/disturbance frequency [8]–[17]. Two solutions have been widely discussed in the literature to overcome this problem and are known as *adaptive repetitive control* [18]–[20] and *high order repetitive control* [21], [22]. The adaptive RC maintains its periodic performance by adapting its sampling frequency to the change in exogenous signal frequency. While on the other hand, HORC controls the issue as mentioned above by supplying comparatively large gain in the neighborhood of the tuned frequency and its multiples. The proposed research work is focused on the design of HORC.

Both the conventional and HORC are used as plug-in devices and have three components, i.e., *a periodic signal generator*, *a low-pass filter,* and *a stabilizing compensator* [23]–[25]. The periodic signal generator offers high gain at the tuned frequency and its harmonics. The low-pass filter attenuates the gain at higher harmonics to make the stability conditions less stringent. Moreover, the stabilizing compensator is used to stabilize the overall repetitive control system. The difference between the conventional and HORC is that

The associate editor coordinating the review of this manuscript and approving it for publication was Jenny Mahoney.

of the periodic signal generator. The periodic signal generator used by n[th] order repetitive controller has 'n' memory loops.

The stability conditions for the "*conventional*" and "*higher-order repetitive*" controller suggest that the inverse of the closed-loop system without RC can be exploited as a stabilizing compensator [9], [26]. However, the inverse model compensator is impossible to use for the non-minimum phase systems and for those systems, which are prone to significant parameter variations. A solution to this crucial problem is the linear phase lead compensator. Zhang et al. proposed this compensator for conventional RC [9]. The same research extends the idea of linear phase lead compensator to HORC. In [26], [27], the improved RC is presented. However, the performance of the RC degrades under frequency variations. In [28], the novel weight selection criteria based HORC for non-minimum phase plants is presented. Authors in [8] have adopted a method for the high-order repetitive control system to further improve the robustness against the uncertainties in the period of signals. However, the robustness discussed in [8] with other modeling uncertainty degrades with increasing order of RC. Secondly, there is a tradeoff between performance and robustness in choosing the order of RC, cutoff frequency, and gain used in control, which is not the case in our design. While the authors in [10], are mainly concerned about saving the memory space and computational burden while keeping the same performance of the conventional system and the proposed system, which is also a significant difference from our design, which has all the merits of above two references and giving good quality of the signal.

To emphasize the originality and contribution of our approach, we re-organize our technical contribution as follows in the introduction. The main contributions of the presented research work are as follows;

- In this paper, the robust HORC with phase lead compensator is proposed. The plant model is non-minimum phase system. The zero-phase tracking error compensator It is proved by simulations as well as validated experimentally that the disturbances are completely rejected by the proposed design. Repetitive controllers have been proposed in recent works [8]–[12], with many notable results on the area, they have improved results in terms of frequency changes in the exogenous signal but a computational burden.
- In the proposed design, the detailed stability conditions are derived analytically and verified by simulations and validated experimentally. No such results are seen in the current research literature.
- To recognize the drawback and limitation of existing research literature [1]–[5], the performance is compared with conventional RC under frequency variations. The proposed design is computationally efficient and always gives superior performance in terms of disturbance frequency rejection accuracy.

The remaining search paper is presented as a short summary of the HORC, and its comparison to the conventional RC is discussed in Section II. The stability conditions for the designed HORC developed in Section III, and the proof of the stability condition theorem is provided in appendix A. In Section IV, the implementation of HORC is given. The performance comparison of the designed controller is presented in Section V and follow on the conclusion of the presented work.

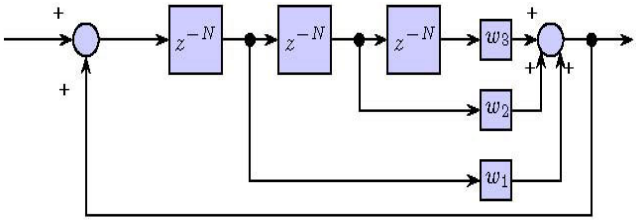

FIGURE 1. Structure of the third-order periodic signal generator.

II. HIGHER ORDER REPETITIVE CONTROLLER

Steinbuch proposed HORC in [19] and present the solution of the crucial problem of performance degradation under frequency variation. The difference between a conventional and HORC is that of the periodic signal generator. The periodic signal generator, used by the HORC, offers relatively high gains in the neighborhood of tuned frequency and its harmonics. Similar to the conventional repetitive control system, HORC system requires a low-pass filter and a stabilizing compensator for stable operation.

A. HIGHER-ORDER PERIODIC SIGNAL GENERATOR

Instead of using one memory loop, the higher-order generator uses multiple weighted memory loops. Figure 1 shows the structure of the third-order periodic signal generator. A general higher-order periodic signal generator is given by the following equations.

$$G_{ho} = \frac{W(z)}{1 - W(z)}, \tag{1}$$

where,

$$W(z) = \sum_{l=1}^{m} w_l z^{-lN}, \tag{2}$$

where N denotes the number of samples in a period,

$$N = \frac{T_P}{T_S}, \tag{3}$$

where T_s gives the time of sampling in the discrete domain, T_P represents the signal period to be produced, m gives the order of the periodic signal generator, w_l is the weight of l^{th} memory loop. The frequency response of the higher-order generator is highly dependent on these weights.

1) CALCULATION OF WEIGHTS w_l

The method described in this Section to calculate the weights follow the reasoning in [19], [29]. The objective is to find such weights so that the higher-order periodic signal generator

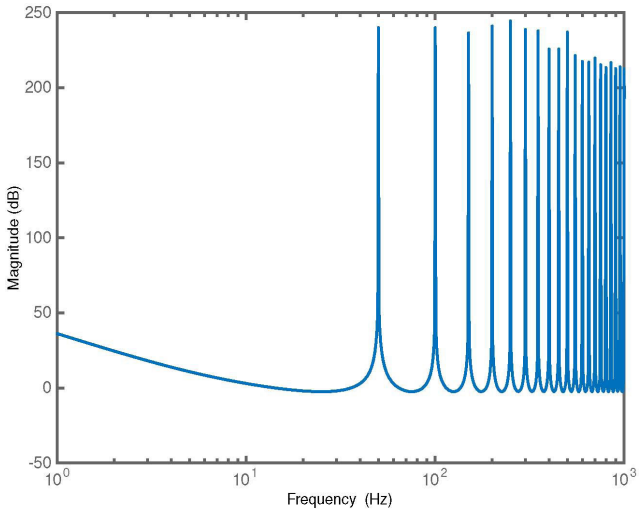

FIGURE 2. Magnitude frequency response of second order periodic signal generator.

gives infinite gain at the tuned frequency and its harmonics. This can be achieved by making the value of $W(z)$ equal to 1 and its first $W(z)$ derivatives equal to 0 at the tuned frequency and its harmonics. It is evident from (1) that $G_{ho}(z)$ has infinite gain when $W(z) = 1$. The mth order generator, the weights can be found by using the following two equations:

$$\sum_{l=1}^{m} w_l = 1 \tag{4}$$

and

$$\sum_{l=1}^{m} w_l l^p = 0 \quad \text{for } p = 1, 2, 3, \ldots, m-1 \tag{5}$$

Using these formulae, the weights for second-order periodic signal generator are evaluated.

$$w_1 = 2 \quad \text{and } w_2 = -1 \tag{6}$$

Similarly, the weights for the 3rd order generator are:

$$w_1 = 3, w_2 = -3 \quad \text{and } w_3 = 1 \tag{7}$$

2) FREQUENCY RESPONSE

The magnitude frequency response of a second-order periodic signal generator is shown in Fig. 2. From this figure, the response of the second-order generator looks almost the same as that of the first-order generator. Similar to the first-order periodic signal generator it has very high gain at the tuned frequency and its harmonics. However, the advantage of higher-order generator becomes evident when its magnitude frequency response is compared with that of the first-order periodic signal generator in the neighborhood of tuned frequency. Figure 3 shows the magnitude frequency response of first, second, and third-order periodic signal generators in the vicinity of tuned frequency, which is 50 Hz. It is shown that at 1 percent variation from tuned frequency, the 3rd order generator gives a gain of about 160 dB, whereas the first-order

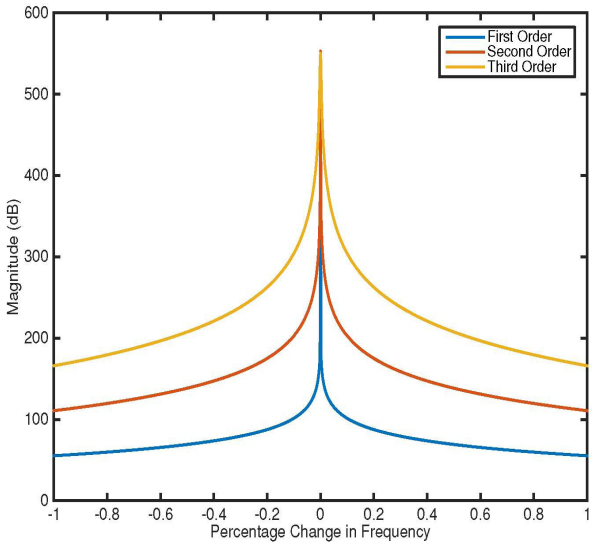

FIGURE 3. Comparison of the magnitude frequency response of first-third order periodic signal generators in the neighborhood of tuned frequency 50 Hz.

generator gives a gain of only 50 dB. Besides, the gain of the second-order generator is about 110 dB.

B. STRUCTURE OF HORC

The HORC is used as a plug-in device and is shown in Fig. 4. Plug-in means that the closed-loop system without the repetitive controller is made stable by designing a conventional proportional integral and derivative (PID) controller, and then the RC is added to the loop. The system response without RC is given by;

$$T_{cl}(z) = \frac{G_c(z)G_p(z)}{1 + G_c(z)G_p(z)} \tag{8}$$

The internal structure of RC is shown in Fig. 5. In addition to the higher-order periodic signal generator, it comprises of a low-pass filter $Q(z)$ and a stabilizing compensator $G_x(z)$. The low-pass filter attenuates gain at higher harmonics, thus making the stability conditions less stringent. The most suitable choice for $Q(z)$ is the first order non-causal finite impulse response filter. It has 0 dB gain at low frequencies and has zero-phase and is expressed as;

$$Q(z) = 0.25z + 0.5 + 0.25z^{-1} \tag{9}$$

$G_x(z)$ is used as a stabilizing compensator. It must be designed in such a way that the HORC does not destabilize and degrade the performance of the loop to which it is added.

C. STABILITY CONDITIONS FOR HORC

Stability conditions for the HORC system shown in Fig. 4 are given by *Theorem I*. *Theorem I* is formulated and derived from [25].

Theorem 1: The repetitive control system presented in Fig. 4 is stable only if it fulfills the following requirements;

1) $T_{cl}(z)$ in (1) shows stable condition.
2) $\|(T_{cl}(z)G_x(z) - 1)Q(z)\mathrm{W}(z)\|_\infty < 1$

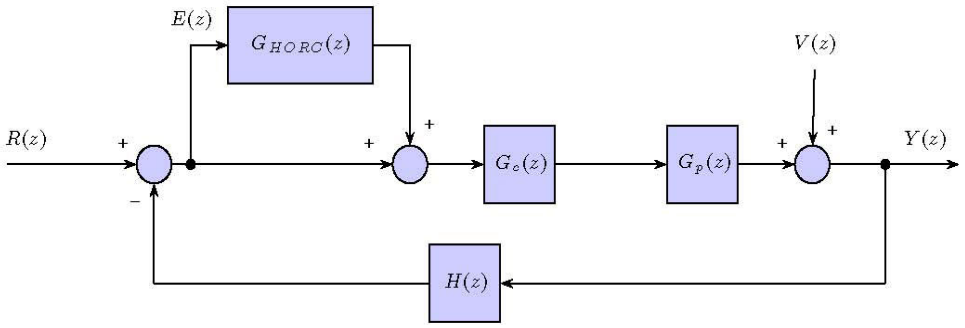

FIGURE 4. Block diagram of a generic closed-loop control system, including the plug-in RC.

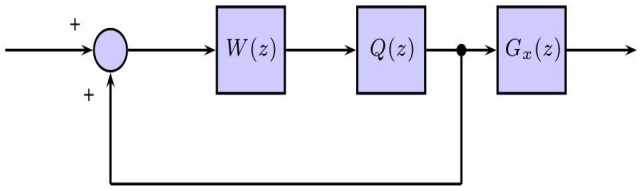

FIGURE 5. Internal structure of the HORC showing plug-in.

By using $Q(z)$ given by (9) and $G_x(z) = K_r/T_{cl}(z)$, the repetitive control system can be quickly stabilized. However, in many cases where the plant is a non-minimum phase, or its dynamics are not adequately modeled, it becomes impossible to use the inverse of $T_{cl}(z)$ as the stabilizing compensator.

In Section III, the above problem is solved by proposing the use of linear phase lead compensator for HOR control system.

III. PHASE LEAD COMPENSATOR

Phase lead compensator [27] is given by the use of linear phase lead compensator for HORC system.

$$G_x(z) = K_r z^m \tag{10}$$

This compensator has two components: K_r and z^m where K_r is the gain element, which has zero phase and z^m is the phase element, which has unity gain and m is a positive integer. The frequency response of $G_x(z)$ is given by:

$$G_x(e^{j\Omega}) = e^{jm\Omega} \tag{11}$$

where

$$\Omega = \omega T_s$$

Thus, the phase $G_x(z)$ is given by:

$$\theta_{G_x} = m\omega T_s \tag{12}$$

The phase in degrees is given by:

$$\theta_{G_x} = m\omega T_s \frac{180^o}{\pi} = m\omega \frac{180^o}{\omega_N} \tag{13}$$

where ω_N is the Nyquist frequency, which is equal to the half of the sampling frequency. This equation shows that the lead compensator has a linear phase, which is zero at $\omega = 0$ and $180^o m$ at $\omega = \omega_N$. The frequency phase response of $G_x(z)$ is shown in Fig. 6.

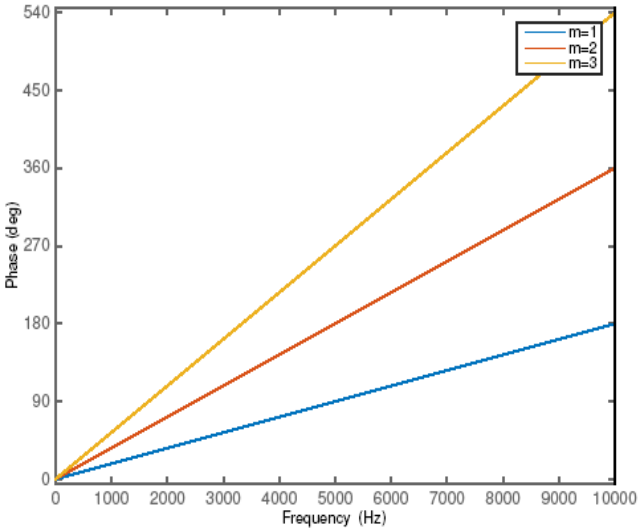

FIGURE 6. Frequency response of $G_x(z)$ for various values of m. Note that both axes have linear scales.

In order to understand how phase lead compensator stabilizes the repetitive control system, the stability conditions in *Theorem, I* need further analysis. If requirement 1) in *Theorem I* is satisfied by appropriate design of $G_c(z)$, then the stability of repetitive control is given by:

$$\|(T_{cl}(z)G_x(z) - 1)Q(z)W(z)\|_\infty < 1 \tag{14}$$

The condition in (14) is reformulated to the following two conditions, and the detailed step-by-step derivation is given in *Appendix A*.

$$\left|m\Omega + \theta_{T_{cl}}\right| = 0^o \text{ for } 0 < \Omega < \pi \tag{15}$$

$$0 < K_r < \frac{\cos(m\Omega + \theta_{T_{cl}})}{M_{T_{cl}}} = K_u \text{ for } 0 < \Omega < \pi \tag{16}$$

Thus, the stability of the HORC system using the phase lead compensator is given by *Theorem II*.

Theorem II: The repetitive control system presented in Fig. 4 is stable for phase lead compensator given by (10) if it met the following requirements;

1) $T_{cl}(z)$ is stable
2) $\left|m\Omega + \theta_{T_{cl}}\right| = 0^o$ for $0 < \Omega < 1$
3) $0 < K_r < \frac{\cos(m\Omega+\theta_{T_{cl}})}{M_{T_{cl}}} = K_u$ for $0 < \Omega < \pi$

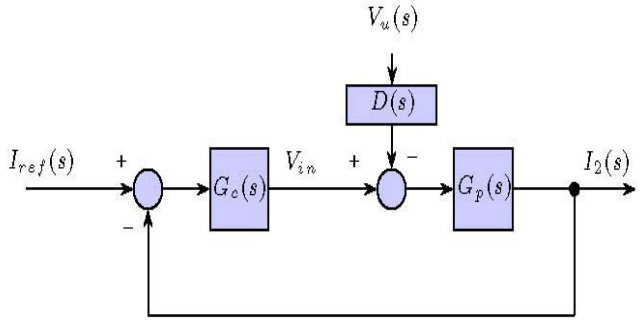

FIGURE 7. Block diagram of the two-level converter with a conventional controller.

These requirements can also be used as a design algorithm. *Requirement 1*: the closed-loop system is made stable using the conventional PID controller in place of $G_c(z)$. *Requirement 2*: is satisfied by a comparison of the sum of the phase angle of the plant and the compensator for various values of m. The comparison gives a suitable value of m. *Requirement 3*: the range of K_r for which the repetitive control system is stable is determined by plotting K_u against frequency. A suitable K_r is then chosen, which gives adequate stability margin.

It should be noted that *Requirement 2* is complicated to achieve for a broad range of frequency. Therefore, it is expected that the stability margins of the HOR control system stabilized by phase lead compensator are small.

IV. CURRENT CONTROL OF TWO-LEVEL CONVERTER

Authors in [29] presented a thorough study of a two-level converter, which is exploited in the proposed research. A block diagram of the two-level converter connected in close-loop is shown in Fig. 7. In Fig. 7, output current $I_2(s)$ of the single phase of the converter and grid voltages $V_u(s)$ are shown. The harmonics enter in the system through this point represented as disturbances. Transfer functions of plant and disturbances are given by;

$$G_p(s) = \frac{1}{(L_1L_2C)s^3 + (K_cL_2C)s^2 + (L_1 + L_2)s} \quad (17)$$

$$D(s) = L_1Cs^2 + K_cCs + 1 \quad (18)$$

Table 1 gives the values of different parameter and component for the two-level converter.

A. CONVENTIONAL PID CONTROLLER

The designing of a PID controller for the two-level converter, the analysis of frequency response is done. The frequency response of transfer functions taken from output current and grid voltage is shown in Fig. 8. It is well defined from the simulation result that the system shows large stability margins as well as large direct current (DC) gain. The system shows a small bandwidth, which is just 398 Hz. A simple proportional controller is employed for improving the bandwidth. The gain is chosen by inspection, and the conventional controller for the two-level converter is;

$$G_c(z) = 3 \quad (19)$$

The frequency response and the designed proportional controller of the converter are presented in Fig. 9. It is seen

TABLE 1. System parameters and component values.

Symbol	Explanation	Value
V_u	Utility phase voltage	230 V (rms)
V_{dc}	DC link voltage	750 V dc
L_1	First Inductor of filter	350 µH
L_2	Second Inductor of filter	50 µH
C	Capacitance	160 µF
K_C	Inner loop gain	13
F_s	Switching frequency	8 KHz
F_g	Grid frequency	50 Hz
f_s	Sampling frequency	20 kHz
N	Samples in one period	400
P_{inv}	Rated Power	80 KVA

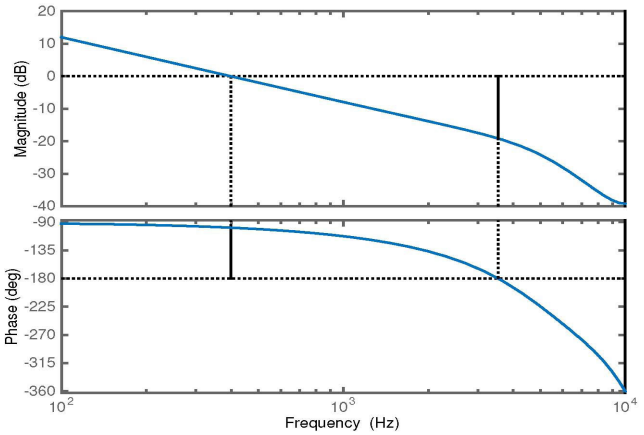

FIGURE 8. Converter transfer function frequency response showing 19.1 dB gain margin, 81.2 degrees phase margin, and 398 Hz bandwidth of the system.

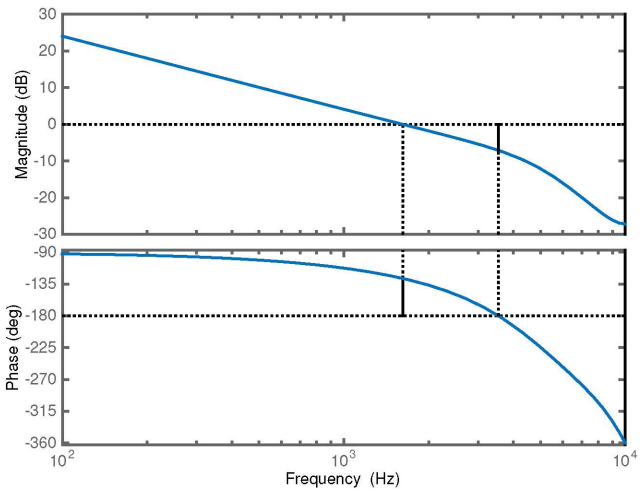

FIGURE 9. The converter's transfer function frequency response along with a proportional controller. It gives 7.11 dB of gain margin, 52.9 degrees of phase margin and 1.62 kHz of the system bandwidth.

from Fig. 9 that the stability margins of the system are still large along with improved bandwidth of 1.62 kHz. Although the system fulfills the desired stability margin, DC gain, and appropriate bandwidth, it still fails on having a large number of harmonic contents, which mean the system is unable to reject the periodic disturbances.

To avert this problem, RC is employed. The detailed design of the RC for the two-level converter and its performance comparison with conventional RC is suggested in [13]. The RC successfully rejects harmonics in the grid, fulfilling the international standards of having a good quality of injected current. Even then, it cannot reject those disturbances due to the grid frequency variations.

B. SECOND-ORDER ODD HARMONIC REPETITIVE CONTROLLER WITH ZERO-PHASE TRACKING ERROR (ZPTE) COMPENSATOR

A robust second-order odd harmonic RC is developed for the two-level converter. Since the converter has a non-minimum phase system, thus, it is hard to employ the inverse model compensator. The zero-phase tracking error (ZPTE) compensator is used to see its effectiveness with HORC. The followed design steps are given below. The details can be found in ref [29].

1. Design a conventional controller $G_C(z)$ such that the closed loop system without RC has large stability margins.
2. Choose an appropriate low pass filter $\|Q(z)\|_\infty \leq 1$.
3. Design a phase compensator which keeps the angle at minimum value within $\pm 90^O$.
4. Find the maximum deviation of $|t_{cl}(\omega) + g_x(\omega)|$ from zero and use it to find the maximum allowable $\|W(z)\|_\infty$ using the method given in [29].
5. Evaluate the weights of HORC
6. Finally, select a suitable $G_x(\omega)$ such that resulting system has fast error convergence.

The second-order RC is expressed as;

$$G_{HORC} = \frac{W(z)Q(z)G_x(z)}{1 - W(z)Q(z)} \tag{20}$$

where,

$$W(z) = w_1 z^{-N} + w_2 z^{-2N} \tag{21}$$

$Q(z)$ is chosen as the low-pass first order non-causal filter.

$$Q(z) = 0.25z + 0.5 + 0.25z^{-1} \tag{22}$$

N is evaluated by the following expression.

$$N = \frac{20000}{50} = 40 \tag{23}$$

The converter is non-minimum phase system; thus, an inverse model compensator cannot be used. Instead, a ZPTE inverse compensator is used [19]. The compensator is given by:

$$G_x(z) = K_r T_{cl} * (z) \tag{24}$$

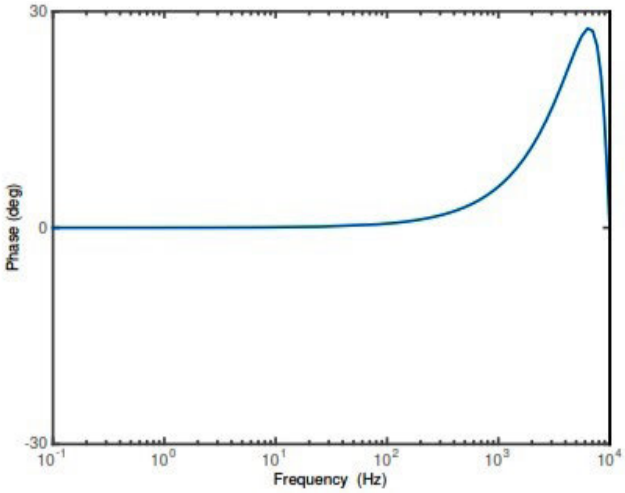

FIGURE 10. Frequency phase response of plant transfer function along with ZPTE compensator.

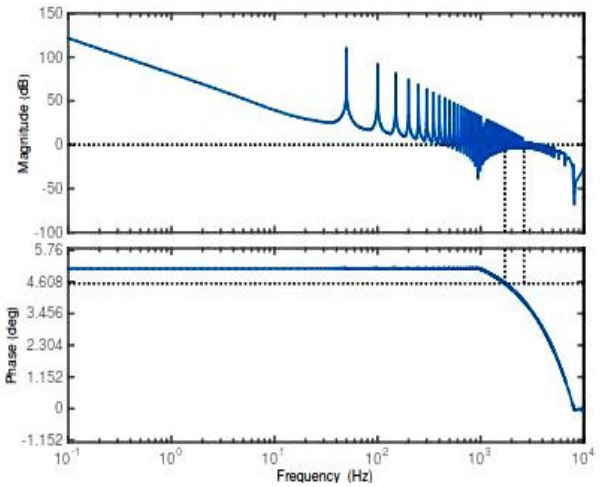

FIGURE 11. Frequency response of the converter transfer function along with designed 2nd order higher order.

where, $T_{cl} * (z)$ is the inverse of $T_{cl}(z)$ excluding the unstable zero. The K_r is a constant factor which is used to satisfy stability conditions. It also controls the error convergence rate.

The frequency response of the converter transfer function with ZPTE compensator is given in Fig. 10. This figure shows the angle $t_{cl}(\omega) + g_x(\omega)$ is within limits of $\pm 90^o$. The maximum deviation of $|t_{cl}(\omega) + g_x(\omega)|$ from zero is 30^0. Thus, the allowable value of $\|W(z)\|_\infty$ is 2.

In final step, the weights are evaluated using method given in [29]. The values of weights are 1.366 and -0.366. The K_r is selected to be 0.8 for fast error convergence.

The phase lead compensator $K_r z^m$ is designed by satisfying the requirements of *Theorem II*. Requirement 1 is satisfied by making the closed-loop system without the repetitive controller stable with $G_c(z) = 3$. It has already been shown that $T_{cl}(z)z^m$ has large stability margins for $G_c(z) = 3$.

The Frequency response of the converter transfer function along with designed 2nd order higher order is shown

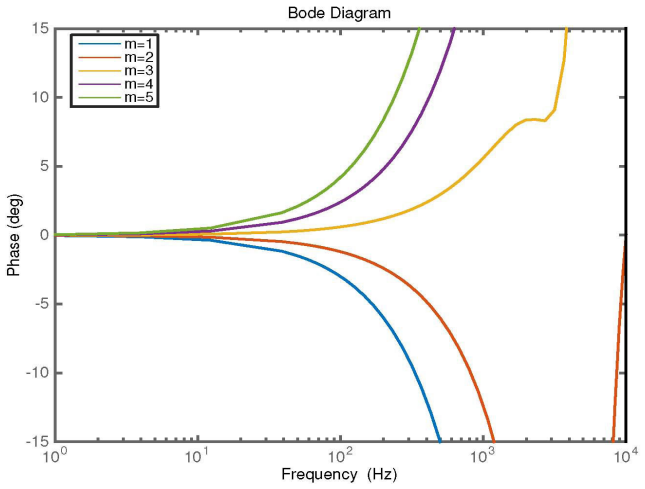

FIGURE 12. Frequency phase plot of $T_{cl}(z)z^m$ for various values of m.

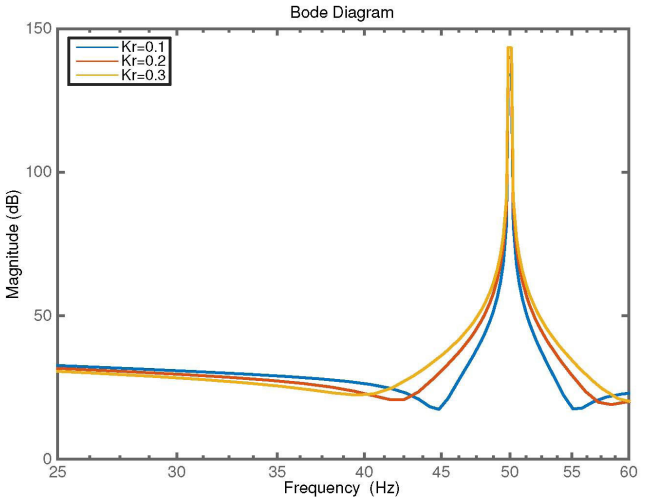

FIGURE 13. Frequency magnitude plot of K_u. The minimum value of K_u is 1.

in Figure 11. The gain margin is 3.6dB and phase margin is 29°.

1) SELECTION OF m

In order to satisfy the second requirement of *Theorem II*, an appropriate value of m has to be selected. This selection is made by comparing the phase of $T_{cl}(z)z^m$ for various values of m. Figure 11 shows a plot of the phase of $T_{cl}(z)z^m$ for different values of m. From Fig. 12, it is evident that the phase remains closer to zero for $m = 2$. Thus, 2 is the most suitable value for m. However, it should be noted that this value of m does not satisfy condition 2 for all Ω such that $0 < \Omega < \pi$. Therefore, it is expected that the stability margins of the repetitive control system are microscopic.

2) SELECTION OF K_r

Finally, K_r is selected from condition 3. Figure 13 shows a plot of K_u against frequency. The minimum value of K_u is 1. Thus, K_r can be selected in the range (0,1). The exact value of K_r is chosen so that the repetitive control system

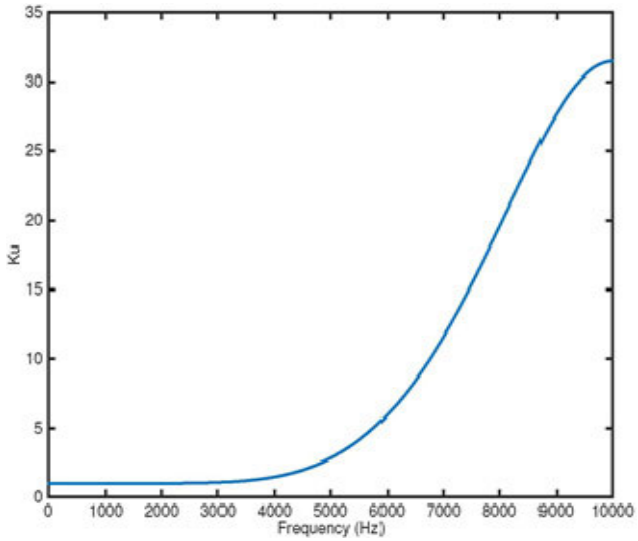

FIGURE 14. Frequency magnitude plot of converter along with the second order RC for different values of K_r.

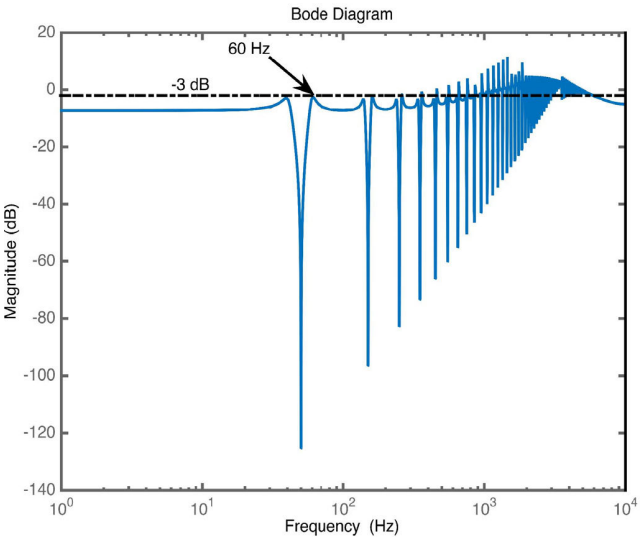

FIGURE 15. Frequency response of the disturbance transfer function. System bandwidth is about 60 Hz.

has maximum stability margins. A smaller value of K_r gives higher stability margins. However, the value of K_r also affects the gain of the repetitive controller at and around the tuned frequency and its harmonics. Figure 14 shows a comparison of different value of K_r. From Fig. 14, it is clear that a smaller value of K_r means that the gain of the repetitive controller at and around the tuned frequency is smaller. Moreover, a smaller gain results in poor disturbance rejection and tracking. Therefore, a compromise value of K_r has to be selected, which gives adequate stability margin along with desired gain at and around the tuned frequency. By this reasoning, K_r is selected as 0.3.

Figure 15 shows the frequency response of the converter's disturbance transfer function for the second-order RC. The bandwidth of the system is only 60 Hz. However, it should be noted that the low bandwidth does not degrade the periodic

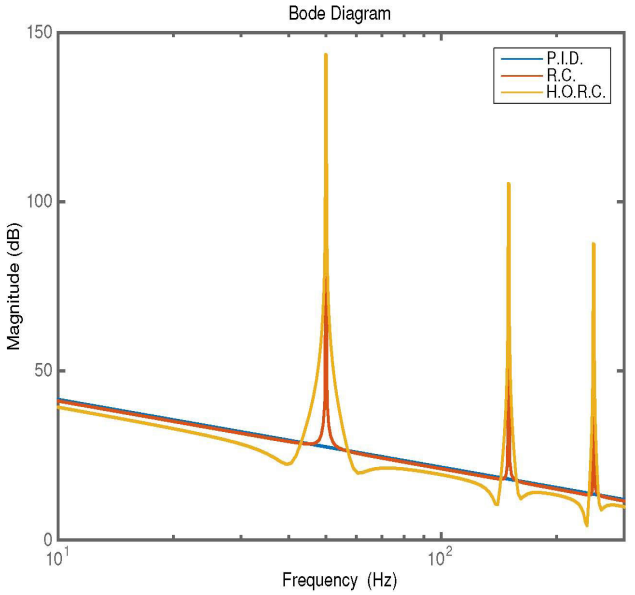

FIGURE 16. Magnitude frequency response of two-level converter transfer function along with various controllers.

TABLE 2. Comparison of output current THD for different controllers.

No.	Controller	Current THD at 50 Hz	Current THD at 49.5Hz
1	PID controller	10.38%	10.38%
2	Repetitive controller	0.23%	10.56%
3	2nd order repetitive controller with ZPTE Compensator	0.04%	2.18%

performance of the system as the system has high attenuation at the tuned frequency and its harmonics. It only degrades the non-periodic performance. The degradation in non-periodic performance means that the settling time and rise time of the system are weak, and the system might have a steady-state error.

V. RESULTS

The magnitude frequency response of the two-level converter controlled by conventional PID, odd harmonic RC, and the proposed second-order HORC is presented in Fig. 16. The parameters are given in Table 1. The mathematical model of system is similar to [13]. The HORC offers substantially high gain at and around the tuned frequency 50 Hz and its harmonics. Thus, it is expected that the HORC performs much better under frequency variation as compared to the other two controllers. All the three controllers are investigated and analyzed employing the linear model of the two-level grid-connected converter. The simulations are done using MATLAB/SIMULINK, assuming the following conditions.

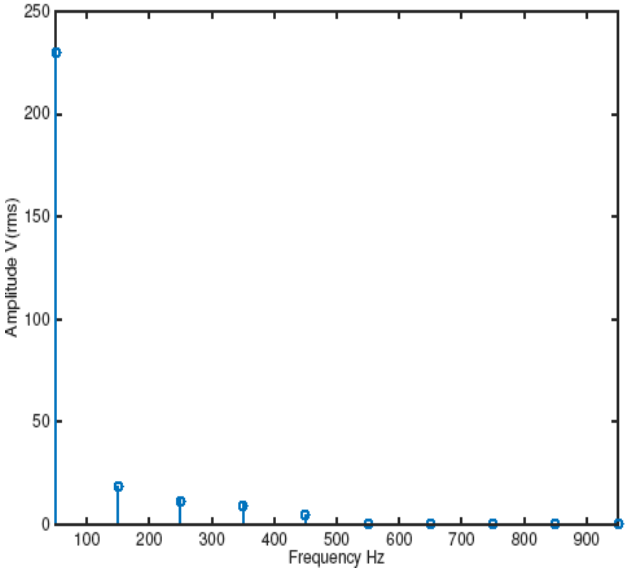

FIGURE 17. Harmonic content in grid voltage showing 10.44% THD.

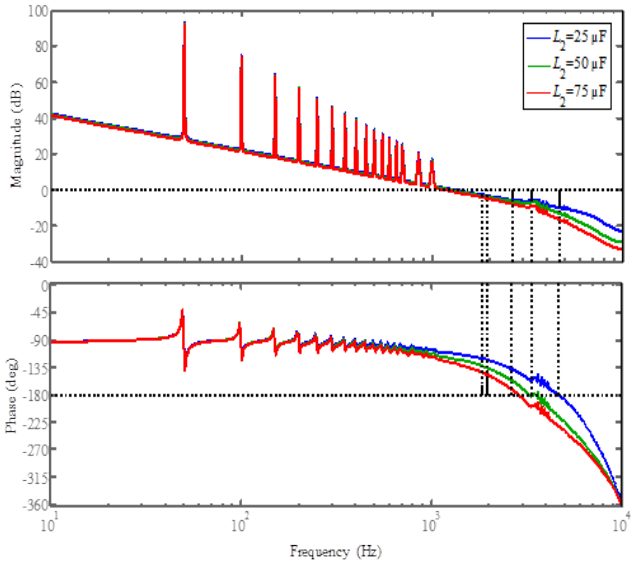

FIGURE 18. Bode diagram showing the effect of variations in L_2 on overall RC system.

1) Reference current and frequency are considered as 100 A and 50 Hz, respectively.
2) The grid voltage shows high harmonic content as the magnitude is presented in Fig. 17. The total harmonic distortion (THD) is 10.44%.
3) The grid frequency variation of 1% is permitted.
4) The grid frequency variation of 1% is permitted.

The output current THD of two-level converter for various controllers assuming different conditions of grid voltage is given in Table 2. According to the standards provided by the institution of electrical and electronics engineers (IEEE) in [27], the current THD must be smaller than 5%. It can be noticed from Table 2 that the PID controller fails to fulfill the required standard in higher harmonics contents of the grid frequency. The conventional odd harmonic RC

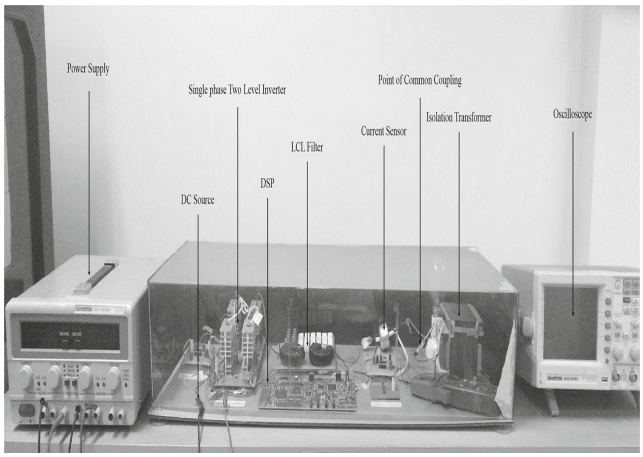

FIGURE 19. Laboratory prototype of two-level single-phase grid inverter.

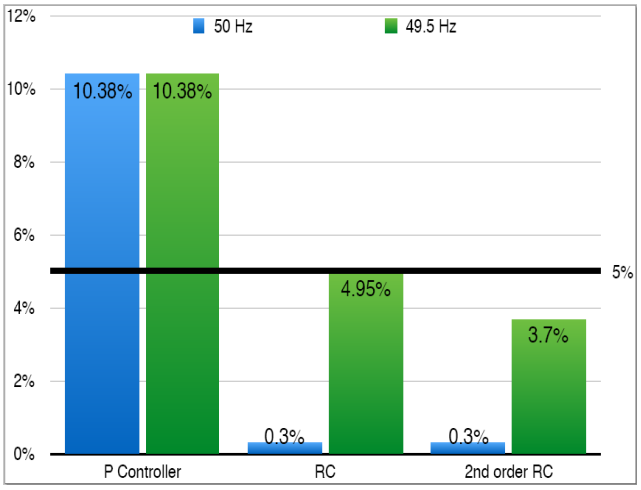

FIGURE 20. Comparison of the output current THD for different controllers under variation in grid frequency. The grid voltage THD is 10.44% (Worst Case Scenario).

successfully removes harmonics having the same conditions. However, it fails on 1% changes in the grid frequency. Whereas, the HORC completely removes harmonics even in the presence of grid frequency variations.

To test the effectives and robustness of proposed approach, the plant model is varied and investigated. The value of the inductor, which is determined by the utility impedance, can vary significantly depending on the site where the converter is installed. To assess the robustness of the system, the uncertainty in the value of L_2 is varied by $\pm 50\%$ and it is observed that the system is always stable having high enough gain and phase margins. It can be concluded that the HORC system can handle variations in utility impedance very well as shown in Figure 18. Thus, the system is robust against uncertainties in utility impedance variations.

To validate the simulation results, a small-scale laboratory prototype of a single-phase utility converter has been used. This converter supports output current up to 10A (rms). Texas instrument DSP model TMS320C6713 was used to implement the proposed RC. Fig. 19 shows the Laboratory prototype of two-level single-phase grid inverter with LCL filter.

Figure 20 shows the output current THD of the two-level converter for different controllers under variations in grid frequency. It depicts that the proportional controller fails to meet the required standards. The conventional odd harmonic repetitive controller successfully rejects harmonics under the same conditions. However, it fails when the grid frequency changes by 1%. Whereas the higher order repetitive controller successfully rejects harmonics even in the presence of variation in grid frequency.

VI. CONCLUSION

The proposed research of phase lead compensator to design higher-order repetitive controller is presented. The stability conditions for the proposed control scheme were derived and analyzed. The designed scheme was applied to the current control of two-level three-phase grid-connected converter. The plant is non-minimum phase system, which uses zero-phase tracking error compensator provides accurate compensation both in terms of phase and magnitude. The performance is compared with conventional RC under frequency variations. Simulation and experimental results showed that the proposed controller outperforms the conventional repetitive controller under variations in grid frequency. The designed HORC successfully removes the variations, and it shows less computational burden. It can be easily concluded that zero-phase error compensator gives promising results with HORC as well.

APPENDIX

DERIVATION OF STABILITY CONDITIONS

$$\left\|(T_{cl}(z)K_r z^m - 1)Q(z)\mathrm{W}(z)\right\|_\infty < 1 \tag{25}$$

Writing this condition in the frequency domain and using the definition of infinity norm following inequality is obtained

$$\left|(1 - M_{T_{cl}}(\mathrm{e}^{j\Omega})\mathrm{e}^{j\theta_{T_{cl}}(\mathrm{e}^{j\Omega})}K_r\mathrm{e}^{jm\Omega})M_Q(\mathrm{e}^{j\Omega})\mathrm{e}^{j\theta_Q(\mathrm{e}^{j\Omega})}M_W(\mathrm{e}^{j\Omega})\mathrm{e}^{j\theta_W(\mathrm{e}^{j\Omega})}\right| < 1 \text{ for } 0 < \Omega < \pi \tag{26}$$

All the frequency responses are functions of $e^{j\Omega}$. In the above equation, this is shown explicitly. Dropping this notation makes the above expression simpler to deal with.

$$\left|(1 - M_{T_{cl}}K_r\mathrm{e}^{j(m\Omega+\theta_{T_{cl}})})M_Q(\mathrm{e}^{j\Omega})\mathrm{e}^{j\theta_Q}M_W\mathrm{e}^{j\theta_W}\right| < 1 \text{ for } 0 < \Omega < \pi \tag{27}$$

Introducing new variable β.

$$\beta = m\Omega + \theta_{T_{cl}} \tag{28}$$

Substituting β in (26) gives:

$$\left|(1 - M_{T_{cl}}K_r e^{j\beta})M_Q e^{j\theta_Q}M_W e^{j\theta_W}\right| < 1 \text{ for } 0 < \Omega < \pi \tag{29}$$

Multiplication inside the parentheses gives:

$$\left|(M_Q M_W e^{j\theta_Q} e^{j\theta_W} - M_Q M_W M_{T_{cl}} K_r e^{j(\beta+\theta_Q+\theta_W)}\right| < 1 \quad \text{for } 0 < \Omega < \pi \tag{30}$$

As

$$e^{j\alpha} = \cos\alpha + j\sin\alpha \tag{31}$$

Thus

$$\left|\begin{array}{l}(M_Q M_W \cos(\theta_Q+\theta_W) + jM_Q M_W \sin(\theta_Q+\theta_W) \\ -M_Q M_W M_{T_{cl}} K_r \cos(\beta+\theta_Q+\theta_W) \\ -jM_Q M_W M_{T_{cl}} K_r \sin(\beta+\theta_Q+\theta_W)\end{array}\right| < 1 \quad \text{for } 0 < \Omega < \pi \tag{32}$$

Taking the absolute value and squaring both sides give:

$$\begin{aligned}&\left[(M_Q M_W \cos(\theta_Q+\theta_W) - M_Q M_W M_{T_{cl}} K_r \cos(\beta+\theta_Q+\theta_W)\right]^2 \\ &+\left[M_Q M_W \sin(\theta_Q+\theta_W) - M_Q M_W M_{T_{cl}} K_r \sin(\beta+\theta_Q+\theta_W)\right]^2 \\ &< 1 \quad \text{for } 0 < \Omega < \pi\end{aligned} \tag{33}$$

Squaring and combining terms give:

$$\begin{aligned}&M_Q^2 M_W^2 + M_Q^2 M_W^2 M_{T_{cl}}^2 K_r^2 \\ &- 2M_Q^2 M_W^2 M_{T_{cl}} K_r[\cos(\theta_Q+\theta_W)\cos(\beta+\theta_Q+\theta_W) < 1 \\ &+ \sin(\theta_Q+\theta_W)\sin(\beta+\theta_Q+\theta_W)] \\ &\text{for } 0 < \Omega < \pi\end{aligned} \tag{34}$$

As

$$\cos(x-y) = \cos x \cos y + \sin x \sin y \tag{35}$$

Thus

$$M_Q^2 M_W^2 + M_Q^2 M_W^2 M_{T_{cl}}^2 K_r^2 - 2M_Q^2 M_W^2 M_{T_{cl}} K_r \cos\beta < 1 \quad \text{for } 0 < \Omega < \pi \tag{36}$$

Solving the inequality for K_r and submitting β from (28) gives:

$$0 < K_r < \frac{1 - M_Q^2 M_W^2}{M_Q^2 M_W^2 M_{T_{cl}} K_r} + \frac{2\cos(m\Omega + \theta_{T_{cl}})}{M_{T_{cl}}} \quad \text{for } 0 < \Omega < \pi \tag{37}$$

Case I: $M_Q \geq 1$
As $M_W^2 << 1$, thus (36) becomes

$$0 < K_r < \frac{-M_Q^2 M_W^2}{M_Q^2 M_W^2 M_{T_{cl}} K_r} + \frac{2\cos(m\Omega + \theta_{T_{cl}})}{M_{T_{cl}}} \quad \text{for } 0 < \Omega < \pi \tag{38}$$

Simplification gives:

$$0 < K_r < \frac{-1}{M_{T_{cl}}^2 K_r} + \frac{2\cos(m\Omega + \theta_{T_{cl}})}{M_{T_{cl}}} \quad \text{for } 0 < \Omega < \pi \tag{39}$$

Only considering the right-hand inequality.

$$K_r < \frac{-1}{M_{T_{cl}}^2 k_r} + \frac{2\cos(m\Omega + \theta_{T_{cl}})}{M_{T_{cl}}} \quad \text{for } 0 < \Omega < \pi \tag{40}$$

Rearranging terms.

$$K_r^2 - \frac{2\cos(m\Omega + \theta_{T_{cl}})}{M_{T_{cl}}} K_r + \frac{1}{M_{T_{cl}}^2} < 0 \quad \text{for } 0 < \Omega < \pi \tag{41}$$

This is quadratic inequality. It can be solved by solving the corresponding quadratic equation that is:

$$K_r^2 - \frac{2\cos(m\Omega + \theta_{T_{cl}})}{M_{T_{cl}}} K_r + \frac{1}{M_{T_{cl}}^2} = 0 \quad \text{for } 0 < \Omega < \pi \tag{42}$$

The roots of K_r from this equation are:

$$K_r = \frac{1}{M_{T_{cl}}}\left[\cos(m\Omega + \theta_{T_{cl}}) \pm \sqrt{\cos^2(m\Omega + \theta_{T_{cl}}) - 1}\right] \quad \text{for } 0 < \Omega < \pi \tag{43}$$

For minimal values of $m\Omega + \theta_{T_{cl}}$, $\sqrt{\cos^2(m\Omega + \theta_{T_{cl}}) - 1} = 0$, Thus the following condition is introduced:

$$\left|m\Omega + \theta_{T_{cl}}\right| = 0^o \text{ for } 0 < \Omega < \pi \tag{44}$$

Under this condition, (42) becomes:

$$K_r = \frac{\cos(m\Omega + \theta_{T_{cl}})}{M_{T_{cl}}} \text{ for } 0 < \Omega < \pi \tag{45}$$

Moreover, the corresponding inequality is:

$$K_r < \frac{\cos(m\Omega + \theta_{T_{cl}})}{M_{T_{cl}}} \text{ for } 0 < \Omega < \pi \tag{46}$$

Case II: $M_Q << 1$
As $M_Q^2 M_W^2 << 1$, thus (36) becomes

$$0 < K_r < \frac{1}{M_Q^2 M_W^2 M_{T_{cl}}^2 K_r} + \frac{2\cos(m\Omega + \theta_{T_{cl}})}{M_{T_{cl}}} \quad \text{for } 0 < \Omega < \pi \tag{47}$$

This inequality is satisfied if the following inequalities are satisfied:

$$0 < K_r < \frac{2\cos(m\Omega + \theta_{T_{cl}})}{M_{T_{cl}}} \text{ for } 0 < \Omega < \pi \tag{48}$$

$$\left|m\Omega + \theta_{T_{cl}}\right| < 90^o \text{ for } 0 < \Omega < \pi \tag{49}$$

(47) and (48) are satisfied if (43) and (45) are satisfied. Thus, (43) and (45) are taken as conditions for stability.

ACKNOWLEDGMENT

The authors would like to acknowledge the funding from the Deanship of Scientific Research, Islamic University of Madinah, Kingdom of Saudi Arabia, under the Research Grant No. 28/40.

REFERENCES

[1] L. Cuiyan, Z. Doagchun, and Z. Xianyi, "A survey of repetitive control," in *Proc. IEEE/RSJ Int. Conf. Intell. Robots Syst. (IROS)*, Sendai, Japan, Apr. 2005, pp. 1160–1166.

[2] M. S. Mahmoud, N. M. Alyazidi, and M. I. Abouheaf, "Adaptive intelligent techniques for microgrid control systems: A survey," *Int. J. Electr. Power Energy Syst.*, vol. 90, pp. 292–305, Sep. 2017.

[3] L. Zhou, J. She, and S. Zhou, "Robust H_∞ control of an observer-based repetitive-control system," *J. Franklin Inst.*, vol. 355, no. 12, pp. 4952–4969, 2018.

[4] Z. Shao and Z. Xiang, "High-order repetitive control for discrete-time linear switched systems," *Int. J. Syst. Sci.*, vol. 48, no. 9, pp. 1882–1890, Jul. 2017.

[5] M. Yu and C. Li, "Robust adaptive iterative learning control for discrete-time nonlinear systems with time-iteration-varying parameters," *IEEE Trans. Syst., Man, Cybern., Syst.*, vol. 47, no. 7, pp. 1737–1745, Jul. 2017.

[6] F. Bouakrif and M. Zasadzinski, "High order iterative learning control to solve the trajectory tracking problem for robot manipulators using Lyapunov theory," *Trans. Inst. Meas. Control*, vol. 40, no. 15, pp. 4105–4114, Nov. 2018.

[7] S. Hou, J. Fei, C. Chen, and Y. Chu, "Finite-time adaptive fuzzy-neural-network control of active power filter," *IEEE Trans. Power Electron.*, vol. 34, no. 10, pp. 10298–10313, Oct. 2019.

[8] L. Wang, W. Zhang, J. Na, G. Li, and S. Su, "Robust repetitive control of three-phase inverter system using high order internal model," in *Proc. 35th Chin. Control Conf. (CCC)*, Jul. 2016, pp. 8544–8549.

[9] B. Zhang, K. Zhou, Y. Wang, and D. Wang, "Performance improvement of repetitive controlled PWM inverters: A phase-lead compensation solution," *Int. J. Circuit Theory Appl.*, vol. 38, no. 5, pp. 453–469, 2010.

[10] K. Jaesuk and S. Seung-Ki, "Harmonic currents control of three-phase four-wire grid-connected PWM inverter based on high-order repetitive controller," in *Proc. 9th Int. Conf. Power Electron. ECCE Asia (ICPE-ECCE Asia)*, Jun. 2015, pp. 2161–2166.

[11] D. Li and Y. Ye, "Second-order RC: Analysis, augmentation, and anti-frequency-variation for single-phase grid-tied inverter," *IET Power Electron.*, vol. 11, no. 6, pp. 1128–1134, May 2018.

[12] J.-H. Park and K.-B. Lee, "Performance improvement for reduction of resonance in a grid-connected inverter system using an improved DPWM method," *Energies*, vol. 11, no. 1, p. 113, Jan. 2018.

[13] M. Jamil, U. Rashid, R. Arshad, M. N. Khan, S. O. Gilani, and Y. Ayaz, "Robust repetitive current control of two-level utility-connected converter using LCL filter," *Arabian J. Sci. Eng.*, vol. 40, no. 9, pp. 2653–2670, Sep. 2015.

[14] T. Inoue, M. Nakano, T. Kubo, S. Matsumoto, and H. Baba, "High accuracy control of a proton synchrotron magnet power supply," in *Proc. 8th IFAC World Congr. Control Sci. Technol. Soc.*, Tokyo, Japan, 1981, pp. 3137–3142.

[15] G. A. Ramos, R. Costa-Castello, and J. M. Olm, *Digital Repetitive Control Under Varying Frequency Conditions*. Berlin, Germany: Springer, 2013, pp. 1–159.

[16] G. A. Ramos, J. M. Olm, and R. Costa-Castelloa, "Repetitive control of an active filter under varying network frequency: Power factor correction," in *Proc. 9th Latin Amer. Robot. Symp. IEEE Colombian Conf. Autom. Control*, Oct. 2011, pp. 1–5.

[17] G. A. Ramos, J. M. Olm, and R. Costa-Castello, "Digital repetitive control under time-varying sampling period: An LMI stability analysis," in *Proc. IEEE Int. Conf. Control Appl.*, St. Petersburg, Russia, Jul. 2009, pp. 782–787.

[18] E. Kurniawan, Z. Cao, and Z. Man, "Design of robust repetitive control with time-varying sampling periods," *IEEE Trans. Ind. Electron.*, vol. 61, no. 6, pp. 2834–2841, Jun. 2014.

[19] M. Steinbuch, "Repetitive control for systems with uncertain period-time," *Automatica*, vol. 38, no. 12, pp. 2103–2109, Dec. 2002.

[20] G. Pipeleers, B. Demeulenaere, J. De Schutter, and J. Swevers, "Robust high-order repetitive control," in *Proc. Amer. Control Conf.*, Seattle, WA, USA, Jun. 2008, pp. 1080–1085.

[21] S. Hara, Y. Yamamoto, T. Omata, and M. Nakano, "Repetitive control system: A new type servo system for periodic exogenous signals," *IEEE Trans. Autom. Control*, vol. 33, no. 7, pp. 659–668, Jul. 1988.

[22] M.-C. Tsai and W.-S. Yao, "Design of a plug-in type repetitive controller for periodic inputs," *IEEE Trans. Control Syst. Technol.*, vol. 10, no. 4, pp. 547–555, Jul. 2002.

[23] G. A. Ramos, R. Costa-Castello, J. M. Olm, and R. Cardoner, "Robust high-order repetitive control of an active filter using an odd-harmonic internal model," in *Proc. IEEE Int. Symp. Ind. Electron.*, Bari, Italy, Jul. 2010, pp. 1040–1045.

[24] T. Inoue, "Practical repetitive control system design," in *Proc. 29th IEEE Conf. Decis. Control*, Honolulu, HI, USA, Dec. 1990, pp. 1673–1678.

[25] R. Costa-Castello, G. A. Ramos, J. M. Olm, and M. Steinbuch, "Second-order odd-harmonic repetitive control and its application to active filter control," in *Proc. 49th IEEE Conf. Decis. Control (CDC)*, Atlanta, GA, USA, Dec. 2010, pp. 6967–6972.

[26] M. Jamil, S. M. Sharkh, and M. A. Abusara, "Current regulation of three-phase grid-connected voltage source inverter using robust digital repetitive control," *Int. Rev. Autom. Control (Theory Appl.)*, vol. 4, no. 2, pp. 211–219, 2011.

[27] M. Jamil, "Design and analysis of odd-harmonic repetitive control for three-phase grid-connected voltage source inverter," *Rev. Electr. Eng.*, vol. 89, no. 1, pp. 292–295, 2013.

[28] M. Jamil, "DSP based hardware implementation of repetitive current controller for interleaved grid connected inverter," *Rev. Electr. Eng.*, vol. 89, no. 2, pp. 251–255, 2013.

[29] U. Rashid and M. Jamil, "Design of higher order repetitive controller for non minimum phase plants," in *Proc. Amer. Control Conf. (ACC)*, Boston, MA, USA, Jul. 2016, pp. 7510–7515.

MOHSIN JAMIL (Senior Member, IEEE) received the B.Eng. degree in industrial electronics from NED University, Pakistan, in 2004, two master's degrees from the National University of Singapore and Dalarna University Sweden, in 2008 and 2006, respectively, and the Ph.D. degree from the University of Southampton, U.K., in 2012. He was an Associate Professor with the Department of Electrical Engineering, Islamic University Madinah, Saudi Arabia, and an Assistant Professor with the Department of Robotics and AI, National University of Sciences and Technology (NUST), Islamabad, Pakistan. He is currently an Assistant Professor with the Department of Electrical and Computer Engineering, Memorial University of Newfoundland, St John's, NL, Canada. His research interests include control system design for power electronic converter and mechatronic systems. His additional interests include myoelectric control, system identification, and renewable energy systems for smart grid technologies. He is the author and coauthor of several IEEE publications in different journals and peer-reviewed conferences. He is a recipient of different awards and funding grants. He is an Associate Editor of IEEE Access.

ASIM WARIS graduated in mechatronics engineering from the College of Electrical and Mechanical Engineering, National University of Sciences and Technology (NUST), Pakistan, and the Ph.D. degree in biomedical engineering from the Department of Health and Science Technology, Aalborg University, Denmark. He worked for the Pakistan Space and Upper Atmosphere Research Commission, from 2013 to 2015. He is currently serving as an Assistant Professor with the Biomedical Engineering and Sciences Department, SMME-NUST. He is the principal investigator of the Electromyography and Brain Computer Interface Lab, and works in the area of neural and rehabilitation engineering, human motor learning, biomedical signals processing, and invasive recordings-based myoelectric control for upper limb prosthetics.

SYED OMER GILANI (Senior Member, IEEE) received the Ph.D. degree in electrical and computer engineering from the National University of Singapore, in 2013, and the M.Sc. degree in computer engineering from Sweden, in 2006. From 2006 to 2008, he worked at the Interactive Multimedia Lab, Singapore. He is currently an Assistant Professor with the National University of Sciences and Technology (NUST), Pakistan. His research interests include human–machine interaction and networking and actively consults for industry on various projects.

BILAL A. KHAWAJA (Senior Member, IEEE) received the B.S. degree in computer engineering from the Sir Syed University of Engineering and Technology, Karachi, Pakistan, in 2002, the M.Sc. degree in communication engineering and signal processing from the University of Plymouth, Plymouth, U.K., in 2005, and the Ph.D. degree in electrical engineering from the University of Bristol, Bristol, U.K., in 2010.

From 2003 to 2004, he was a Software Engineer with Simcon International (Pvt.) Ltd., Pakistan. From 2010 to 2016, he was working as an Assistant Professor with the Electronics and Power Engineering Department, PN-Engineering College, National University of Science and Technology (NUST), Karachi, Pakistan. In 2015, he was a Visiting Postdoctoral Researcher with the Lightwave Systems Research Laboratory, Queens University, Kingston, Canada, where he was involved in the Natural Sciences and Engineering Research Council (NSERC)—Canada CREATE Next Generation Optical Network (NGON) project on the characterization and measurements of 25GHz RF signal generation optical comb sources. He is currently an Associate Professor with the Department of Electrical Engineering, Faculty of Engineering, Islamic University of Madina, Medina, Saudi Arabia. He has authored and coauthored several journals and IEEE proceeding publications. His current research interests include next-generation of millimetre-wave (mm-wave) radio-over-fiber and optical communication systems, mm-wave and THz signal generation mode-locked lasers, and RF transceiver design and antennas design/characterization for the Wi Fi/IoT/UAVs/FANETs/5G systems/UWB wireless body area networks, wireless sensor networks, and millimeter-wave frequency bands. He is an active reviewer for many reputed IEEE journals and letters.

MUHAMMAD NASIR KHAN received the B.Eng. degree in electronic engineering from Dawood Engineering University, Karachi, Pakistan, in 2002, the M.Sc. degree (Hons.) in communication engineering, one from the University of Engineering and Technology Lahore, Pakistan, and the other from the Technical University of Delft, The Netherlands, in 2007 and 2009, respectively, and the Ph.D. degree in telecommunication from the Institute for Telecommunication Research, University of South Australia, Australia, in 2013.

He is currently working as a Professor in electrical engineering with the Department of Communication Group, University of Lahore, Pakistan. His research interests include channel coding, detection theory, development of energy efficient algorithm for wireless sensor networks, signal processing for communication, advance metering infrastructure, and optimization techniques. He wrote two books of undergraduate level and is the author of several well-known journals and IEEE proceedings. He is a member of the IEEEP, Pakistan.

ALI RAZA received the B.S. and M.Sc. degrees in electrical engineering from the University of Engineering and Technology, Lahore, Pakistan, in 2010 and 2013, respectively, and the Ph.D. degree in electrical engineering from the Harbin Institute of Technology, Harbin, China, in 2016.

He is currently working with the Department of Electrical Engineering, The University of Lahore, Lahore. He has authored and coauthored several technical journal articles and technical conference proceedings. His research interests include operation and control of M-VSC-HVDC, including its effects on power systems, as well as the protection, optimization, and topological evaluation of MT-HVDC transmission systems for large offshore wind power plants. He has been a TPC member of the International Symposium on Wireless Systems and Networks (ISWSN) since 2017. He received the First Best Paper Award 2014 IEEE International Conference on Control Science and Systems Engineering. He is the Co-Chair of the Asia Pacific International Conference on Electrical Engineering 2019 (APICEE 2019).